In Vivo ^{31}P MRS Imaging of Intracellular NAD Contents and NAD$^+$/NADH Redox States in Normal and Ischemic Brains

Xiao-Hong Zhu[1], Ming Lu[1], Yi Zhang[1], and Wei Chen[1]

[1]*Center of Magnetic Resonance Research, Department of Radiology, University of Minnesota Medical School, Minneapolis, MN, United States*

Introduction Nicotinamide adenine dinucleotide (NAD), a coenzyme and co-substrate found in all living cells, has two basic forms: NAD$^+$ (oxidized form) and NADH (reduced form); the ratio of NAD$^+$/NADH is defined as the intracellular redox state which reflects the fundamental balance of the cellular redox reactions. Intracellular NAD is tightly linked to cellular energy metabolism and various biological processes; thus, ability to study NAD and its redox state is essential for understanding the basis of cellular metabolism and regulation in health and disease [1-3]. However, direct assessment of NAD and NAD$^+$/NADH redox *in vivo* is challenging. In this study, we exploited a novel ^{31}P MRS approach for imaging NAD and its redox state in animal brains at 16.4 Tesla (T). Our results reveal that the MR signals of NAD$^+$ and NADH can be robustly measured and respectively identified in animal brains *in vivo*, thus, the cerebral NAD contents and NAD$^+$/NADH redox state can be quantitatively determined. The feasibility for imaging NAD in normal cat brain was evaluated and the alteration of the NAD concentrations and the redox state in the rat brain underwent an acute ischemic-recovery preparation was also studied.

Methods Anesthetized adolescent cats were scanned under normal physiological condition. Six Sprague Dawley rats with forebrain ischemia-recovery preparation were scanned multiple times under different physiopathological conditions. All MR measurements were conducted at 16.4T/26cm horizontal animal scanner using ^{1}H/^{31}P surface coils. The ^{31}P chemical shift imaging (CSI) data of rat brain were acquired with 87μl nominal resolution and 9 min acquisition time; 52μl nominal resolution and ~1hr acquisition time were used for the cat study. A novel quantification method capable of simulating and/or fitting the resonances of α-ATP, NAD$^+$ and NADH at a given magnetic field strength was applied. The integral of these resonances were compared with that of α-ATP, in which its baseline concentration was set to 2.8mM [4]. Thus, the absolute concentrations of α-ATP, NADH and NAD$^+$ in each animal under different conditions can be determined, along with the NAD$^+$/NADH redox ratio and the total NAD content ($[NAD]_{total}$=[NAD$^+$]+[NADH]) in the brain. All results were presented as mean±standard deviation. Paired student's t-test was used for statistical analysis.

Results Figure 1 displays typical 3D ^{31}P-CSI data of cat brain, including two ^{31}P spectra of individual voxels. Excellent sensitivity and spectral quality at ultrahigh field ensured reliable detection and quantification of the cerebral NAD contents and redox state. The images of NAD$^+$, NADH, total NAD concentrations and the NADH/NAD$^+$ redox ratio from a representative cat brain were shown in Fig. 1B. It was found that the NAD levels and the redox state were relatively uniform in imaged brain regions with mean values of [NAD$^+$]=0.35±0.05mM; [NADH]=0.13±0.03mM; $[NAD]_{total}$=0.49±0.04mM; and NAD$^+$/NADH redox ratio of 2.8±0.8 (sagittal) and 2.8±1.5 (coronal) across the imaging voxels. These results are in general agreement with the biochemical analysis results from extracted brain tissue [5-6]. Figure 2 presents the original and fitted ^{31}P spectra of a representative rat brain under pre-ischemic baseline, forebrain ischemia, post-ischemic recovery and postmortem conditions; and the summarized average results. The alteration of the α-ATP, NADH and NAD$^+$ signals in response to the physiopathological perturbation were clearly evident. It was found that the baseline concentrations of NAD$^+$, NADH, total NAD and the NAD$^+$/NADH redox ratio in anesthetized rat brains were strikingly similar to that of cat brains. During forebrain ischemia, a decrease of ATP was in company with NAD$^+$ reduction and NADH increase, resulting in a profound decrease in the NAD$^+$/NADH redox state. During the post-ischemic recovery, the levels of ATP and NAD$^+$ were restoring and NADH was receding. The alteration in the NAD$^+$/NADH redox state followed the trends of NAD$^+$ but it was more pronounced due to the opposite change in the NADH. It was also found that the total NAD content in the rat brain gradually declined during the repeated ischemic insults and it did not recover in the post-ischemic periods since both NAD$^+$ and NADH levels were lower than that of baseline. The ATP was completely depleted in the postmortem brain while much larger changes in the NAD$^+$, total NAD contents and the redox ratio relative to the live brain were also observed.

Conclusion We report herein that the cerebral NAD$^+$/NADH redox state and the intracellular NAD contents, including NAD$^+$, NADH and total NAD, and their changes can be robustly and non-invasively imaged under normal and physiopathological conditions. This simple and highly applicable MR imaging approach should have great potential for studying the cellular metabolism and redox state in different organs of various animal models, as well as for human applications.

Acknowledgement This works is supported by NIH grants NS057560, NS41262, NS070839, P41 RR08079 & EB015894, S10 RR025031 and P30 NS057091 & NS076408.

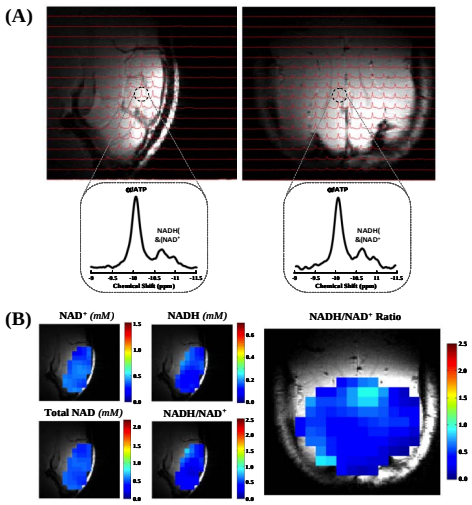

Figure 1. *In vivo* ^{31}P MRS images of the NAD contents and the redox state in normal cat brain. (A) Two examples of ^{31}P-CSI slices in sagittal (left) and coronal (right) orientations extracted from 3D-CSI data were overlaid on corresponding ^{1}H anatomical images. Two ^{31}P spectra of individual voxels are displayed showing excellent spectral quality of α-ATP, NAD$^+$ and NADH; (B) Quantitative analysis of the ^{31}P-CSI data resulted in the images of NAD$^+$, NADH and total NAD contents and the NADH/NAD$^+$ ratio images in the sagittal (left) and coronal (right) orientations, respectively.

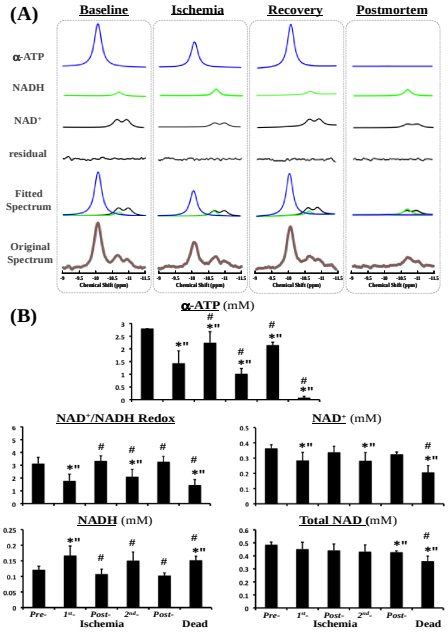

Figure 2. (A) *In vivo* ^{31}P MR spectra and their corresponding fitting results of total NMR signal (red) and individual NAD$^+$ (black), NADH (green) and α-ATP (blue) signals obtained in a representative rat brain under different conditions. (B) Summary of α-ATP and NAD contents and redox states in rat brains under different pathophysiological conditions (Mean ±SD, *n*=6). Paired t-test was used to assess the differences in each parameter at a particular condition with that of baseline (* indicates significant difference with p≈10^{-3}-10^{-6}); and/or at subsequent conditions with that of prior conditions (# indicates a significant difference with p≈10^{-3}-10^{-5}).

References [1] Siesjo, B. K. *Brain Energy Metabolism* (1978); [2] Pollak et al. *Biochem J* **402**, 205-218 (2007); [3] Belenky et al. *Trends Biochem Sci* **32**, 12-19 (2007); [4] Du et al. *PNAS* **105**, 6409-6414 (2008); [5] Lowry et al. *J Biol Chem* **236**, 2746-2755 (1961); [6] Klaidman et al. *Anal Biochem* **228**, 312-317 (1995).